Electrochimica Acta 169 (2015) 283–290

Contents lists available at ScienceDirect

Electrochimica Acta

journal homepage: www.elsevier.com/locate/electacta

Synthesis of ZnO–$ZnCo_2O_4$ hybrid hollow microspheres with excellent lithium storage properties

Qingshui Xie, Deqian Zeng, Yating Ma, Liang Lin, Laisen Wang, Dong-Liang Peng *

Fujian Key Laboratory of Advanced Materials, Collaborative Innovation Center of Chemistry for Energy Materials, Department of Materials Science and Engineering, College of Materials, Xiamen University, Xiamen 361005, China

ARTICLE INFO

Article history:
Received 6 February 2015
Received in revised form 7 April 2015
Accepted 8 April 2015
Available online 9 April 2015

Keywords:
Zinc oxide
Zinc cobalt oxides
Hybrid hollow microspheres
Anodes
Lithium ion batteries

ABSTRACT

ZnO–$ZnCo_2O_4$ hybrid hollow microspheres are successfully produced via an annealing process of the prefabricated zinc–cobalt citrate hollow microspheres in air. ZnO and $ZnCo_2O_4$ have homogeneous distribution within the whole hollow microspheres. The gained hybrid hollow microspheres deliver outstanding lithium storage properties when utilized as the anode material in lithium ion batteries. A high reversible capacity of 1199 mA h g^{-1} can be retained after 200 cycles. The exceptional electrochemical properties of the hybrid hollow microspheres are ascribed to the synergetic effect between ZnO and $ZnCo_2O_4$ nanoparticles, the catalytic effect of Co nanocrystals, the favorable hollow structures together with the nanometer-sized building blocks of hybrid microspheres.

1. Introduction

In the past decades, lithium ion batteries have been deemed as one of the most promising energy storage devices in the fields of portable electronics, electric vehicles and hybrid electric vehicles in terms of their long cycling time, large energy density and no memory effect [1–8]. The traditional graphite anodes could not satisfy the ever-growing large energy requirements in the current society owing to their relatively low theoretical capacity of 372 mA h g^{-1} and safety issue. Seeking for alternative electrode materials has triggered widespread research interest in recent years. Compared to conventional carbonaceous materials, transition metal oxides have been paid great attentions for using as the anode material in lithium ion batteries in view of their higher theoretical capacity [9–18]. Although great progresses have been made, the electrochemical performances of many binary metal oxides are still unsatisfactory due to their intrinsic characteristics including poor electrical conductivity and ion diffusion kinetics together with huge volume variation during the repetitive lithium uptake/removal process. Recently, studies have demonstrated that ternary transition metal oxides with AB_2O_4 spinel structures can address the aforementioned shortcomings to some extent due to the reinforcement or synergetic effect between different constituent. For example, various ternary transition metal oxides including $NiFe_2O_4$, $CuCo_2O_4$, $ZnCo_2O_4$, (Mg, Cu)-codoped $ZnFe_2O_4$ and so on, have been successfully prepared and reveal good electrochemical properties when applied as the anode materials for lithium ion batteries [19–24]. Among them, $ZnCo_2O_4$, the partial replacement of Co element in Co_3O_4 by cheaper and nontoxic Zn element, holds bright prospects as the advanced electrode materials not only because Zn and Co elements can function as mutual favorable buffering matrices to alleviate the large mechanical stress derived from the severe volume change during cycling, but also because Zn can further reversibly react with Li through alloying/dealloying reactions to contribute to extra capacity. Up to date, various $ZnCo_2O_4$ materials such as nanoparticles, nanotubes, yolk–shell microspheres and feather-like nanostructures have been fabricated and employed as the anode materials for lithium ion batteries [22,25–28].

Very recently, mixed metal oxides have been intensively applied as the advanced anode materials for lithium ion batteries since the number of ternary transition metal oxides which have a single phase is greatly limited [29–34]. The synergetic effect between the different metal oxides is helpful in further increasing the lithium storage performances of electrode materials. For example, Fe_2O_3@NiO core/shell nanorod arrays prepared by Tu's group demonstrated better lithium storage properties than individual Fe_2O_3 and NiO electrodes [29]. It was pronounced that the special structural stability could be realized for hybrid nanorod arrays by combining the Fe_2O_3 cores and ultrathin NiO shells, accounting for their superior electrochemical properties. Three-dimensional branched CuO/Co_3O_4 core/shell nanowire

* Corresponding author. Tel.: +86 592 2180155; fax: +86 592 2183515.
E-mail address: dlpeng@xmu.edu.cn (D.-L. Peng).

http://dx.doi.org/10.1016/j.electacta.2015.04.041
0013-4686/

heterostructures were produced by Li's group through a simple thermal oxidation approach, which revealed the greatly enhanced cycling stability on the basis of the synergetic effect between CuO and Co_3O_4 [32]. Unfortunately, most of mixed metal oxides reported previously show the branched configurations and there are few literatures concentrating on the fabrication of mixed metal oxides with hollow structures and their lithium storage properties. In addition, the conventional "two-step" strategy for the fabrication of the mixed metal oxides with branched structures, that is to firstly prepare the core materials combined with subsequent synthesis of shell materials, is complicated and tedious. Consequently, it is of great significance to produce mixed metal oxides with hollow structures through a simple approach, which may demonstrate the exceptional lithium storage properties.

In this work, well-dispersed ZnO–$ZnCo_2O_4$ hybrid hollow microspheres are produced for the first time through an annealing treatment of the pre-synthesized zinc–cobalt citrate hollow microspheres in air. Based on their unique structural features, the prepared hybrid hollow microspheres depict high specific capacity, extraordinary cycling stability and exceptional rate capability when applied as the anode materials for lithium ion batteries. After 200 cycles, well-dispersed ZnO–$ZnCo_2O_4$ hybrid hollow microspheres deliver a high reversible capacity of about 1199 mA h g^{-1} at a current density of 200 mA g^{-1}. The reasons for the excellent lithium storage properties of hybrid hollow microspheres are discussed in detailed.

2. Experimental

2.1. Synthesis

Zinc citrate hollow microspheres were firstly fabricated on the basis of our earlier literature [35]. 30 ml of 0.3 M cobalt nitrate solution containing 0.06 g of zinc citrate hollow microspheres was ultrasonicated for 10 min with subsequently aging treatment at room temperature for 1 h. After that, the pink zinc–cobalt citrate precipitate was acquired, rinsed with deionized water for three times and dried at 70 °C overnight. The weight of the harvested zinc–cobalt citrate hollow microspheres is about 0.0423 g and the yield is 70.5%. By annealing the obtained zinc–cobalt citrate hollow microspheres at 500 °C for 2 h in air, ZnO–$ZnCo_2O_4$ hybrid hollow microspheres (about 0.0311 g) could be obtained.

2.2. Characterizations

X-ray diffraction (PANalytical X'pert PRO x-ray diffractometer, Cu Kα radiation 40 kV, 30 mA), scanning electron microscopy (Hitachi SU-70), transmission electron microscopy (JEM-2100, 200 kV), Fourier-transform infrared test (Nicolet Nexus-670 FT-IR spectrometer), thermogravimetric (TG) measurement (SDT-Q600 thermal analyzer) and the specific surface area evaluations (TriStar 3020 system) were carried out to detailedly characterize the harvested zinc–cobalt citrate precursor and ZnO–$ZnCo_2O_4$ hybrid hollow microspheres.

2.3. Electrochemical evaluations

The anode was prepared by coating a homogeneous slurry containing 70 wt% of ZnO $ZnCo_2O_4$ hybrid hollow microspheres (active materials, 0.21 g), 20 wt% of acetylene black and 10 wt% of poly (vinyl difluoride) (PVDF) to copper foil (d = 16 mm) combined with subsequent drying treatment at 80 °C overnight under vacuum condition. The coating weight of active materials in the working electrode is 1.8–2.0 mg and the geometrical area of the electrode is about 2.01 cm^2. 1 M $LiPF_6$ in ethylene carbonate (EC) and diethyl carbonate (DEC) (1:1, v/v) was applied as the

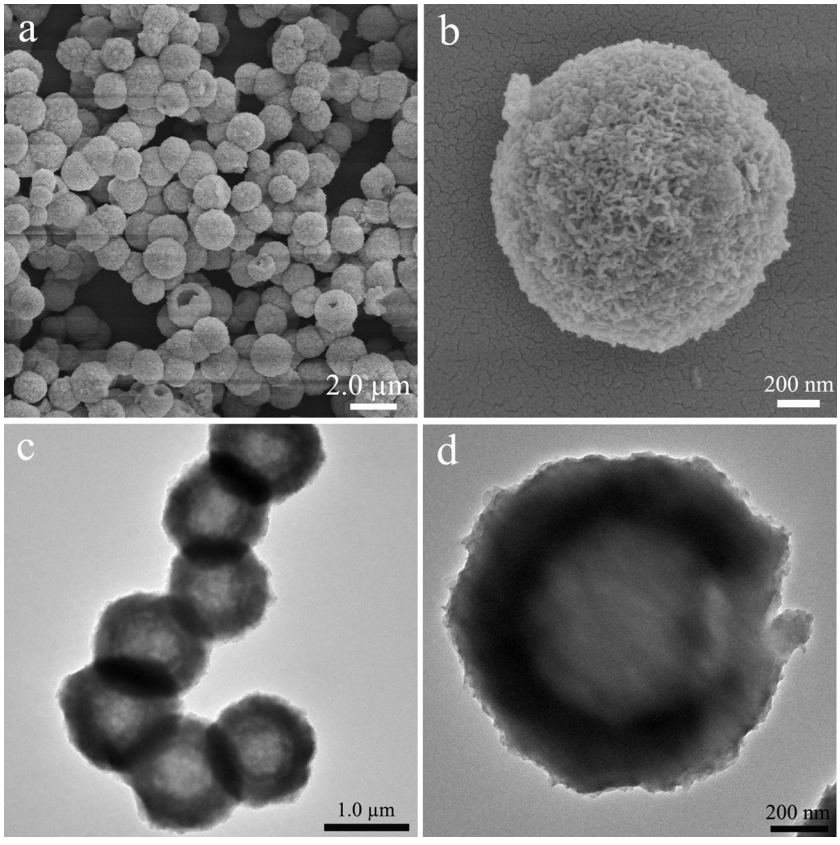

Fig. 1. The SEM (a-b) and TEM (c-d) images of zinc–cobalt citrate hollow microspheres.

electrolyte. Lithium foil and Celgard 2400 respectively serve as the counter and reference electrode, and separator. Coin-type 2025 cells were assembled in a glove box filled with argon. The cycling and rate performances were carried out on a Neware battery tester. Cyclic voltammetry profiles were collected on an Autolab electrochemical workstation.

3. Results and discussion

3.1. Morphology and structure characterizations

Fig. 1 exhibits the SEM and TEM images of the obtained zinc–cobalt citrate precursor. Apparently, the precursor is dominated by the dispersed microspheres with an average diameter of about 1.7 μm (Fig. 1a). The SEM micrograph at a higher amplification factor (Fig. 1b) shows the coarse and loose surface of microsphere. The microspheres contain Zn, Co, O and C elements (Fig. S1), indicating the successful adsorption of cobalt ion on the surfaces of zinc citrate hollow microspheres. The hollow structures of the acquired zinc–cobalt citrate microspheres are testified from the TEM observations (Fig. 1c-d). From XRD pattern, the obtained zinc–cobalt citrate precursor is mainly amorphous (Fig. 2a). FT-IR characterization displayed in Fig. 2b suggests the presence of carboxylate acid groups (—COO^-, peaks around 1574.5 and 1398.2 cm^{-1}) and hydroxide groups (–OH, peak nearby 3424 cm^{-1}) in precursor. With all of above observations in mind, the successful fabrication of zinc–cobalt citrate hollow microspheres can be easily realized through a simple aging process of zinc citrate hollow microspheres in cobalt nitrate solution. The TG measurement of zinc–cobalt citrate hollow microspheres is revealed in Fig. S2. The initial weight loss below 200 °C relates to the loss of moisture in sample and the following large weight loss between 230 and 305 °C is associated with the decomposition of zinc–cobalt citrate to ZnO–$ZnCo_2O_4$ hybrids. Thus, the calcination temperature is determined to be 500 °C, at which zinc–cobalt citrate could be completely transformed to ZnO–$ZnCo_2O_4$ hybrids. XRD pattern (Fig. 2a) of the annealed product reveals the diffraction peaks of hexagonal ZnO (JCPDS card No. 36-1451) and spinel $ZnCo_2O_4$ (JCPDS card No. 23-1390). The lattice parameter (a) of $ZnCo_2O_4$ is calculated to be about 0.81096 nm. In order to further identify the composition of the product acquired after calcination, the obtained hybrid powders were dispersed into 4.0 M NaOH solution and stirred for 6 h to selectively dissolve ZnO. No diffraction peaks resulted from ZnO can be observed from XRD pattern of the product obtained after dissolution treatment (Fig. S3a), suggesting that ZnO has been completely removed from hybrid powders. EDS measurement of the product after dissolution treatment indicates the presence of Zn, Co and O elements with a Zn/Co molar ratio of about 0.5 (Fig. S3b). SEM image (Fig. S3c) shows that the hybrid microspheres have cracked to nanoparticles after dissolution treatment. According to the above results, it is reasonable to pronounce that ZnO–$ZnCo_2O_4$ hybrids can be successfully prepared by calcination of zinc–cobalt citrate precursor in air and $ZnCo_2O_4$ nanoparticles can be harvested by selectively removal of ZnO from ZnO–$ZnCo_2O_4$ hybrids. According to the Scherrer equation, the main crystal sizes of ZnO and $ZnCo_2O_4$ particles are determined to be 12.2 and 11.3 nm, respectively.

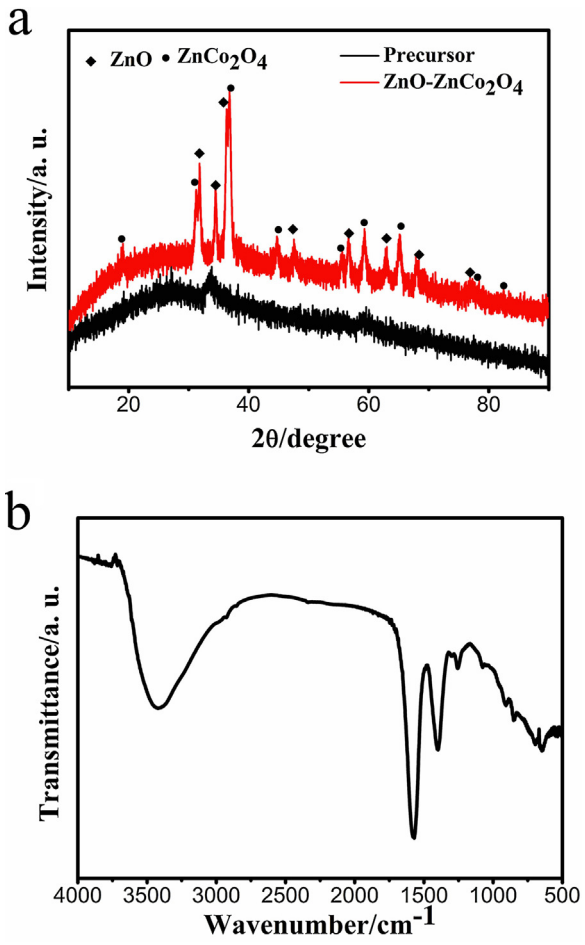

Fig. 2. (a) The XRD patterns of zinc–cobalt citrate hollow microspheres and ZnO–$ZnCo_2O_4$ hybrid hollow microspheres. (b) FT-IR spectrum of zinc–cobalt citrate hollow microspheres.

SEM image displayed in Fig. 3a depicts that the product acquired after calcination consists of a large quantity of dispersed microspheres. From the careful SEM observations (Fig. 3b-c), the microspheres are made up of many ZnO and $ZnCo_2O_4$ nanoparticles with an average particle size of around 30 nm. ZnO and $ZnCo_2O_4$ nanoparticles contact with each other closely. The hollow structures of hybrids are perfectly maintained after heating treatment, which is evidenced from the cracked microsphere (the inset in Fig. 3a) and TEM observations (Fig. 3d-e). From high resolution TEM (HRTEM) image (Fig. 3f), the interplanar spacings are calculated to be 0.260 and 0.243 nm, which are in line with the (0 0 2) plane of ZnO and (3 1 1) plane of $ZnCo_2O_4$, respectively. Scanning TEM (STEM) image and the corresponding element mappings are revealed in Fig. 3g-j, from which the uniform distribution of Zn, Co and O elements can be observed clearly. Namely, ZnO and $ZnCo_2O_4$ nanoparticles homogeneously distribute within the whole hollow microspheres and contact with each other intimately. It is worth pointing out that the homogeneous distribution of different components in mixed metal oxides plays a key role in obtaining good lithium storage performances. The weight ratio of ZnO/$ZnCo_2O_4$ in the hybrid microspheres is calculated to be 1.04 from EDS measurement (Fig. S4). The BET surface area of ZnO–$ZnCo_2O_4$ hybrid hollow microspheres is 26.2 $m^2 g^{-1}$ determined from N_2 adsorption–desorption evaluation at 77 K (Fig. S4). The pore size distribution implies the presence of mesopores centered at 25.5 nm (the inset in Fig. S5).

According to above observations and discussions, the successful preparation of well-dispersed ZnO–$ZnCo_2O_4$ hybrid hollow microspheres through a simple strategy is schematically illustrated in Fig. 4. During the aging process of zinc citrate hollow microspheres in cobalt nitrate solution, cobalt ions are capable of adsorbing on the surfaces of zinc citrate hollow microspheres by means of the electrostatic interplay between the positive cobalt ions and negative carboxylate acid groups (—COO^-), resulting in

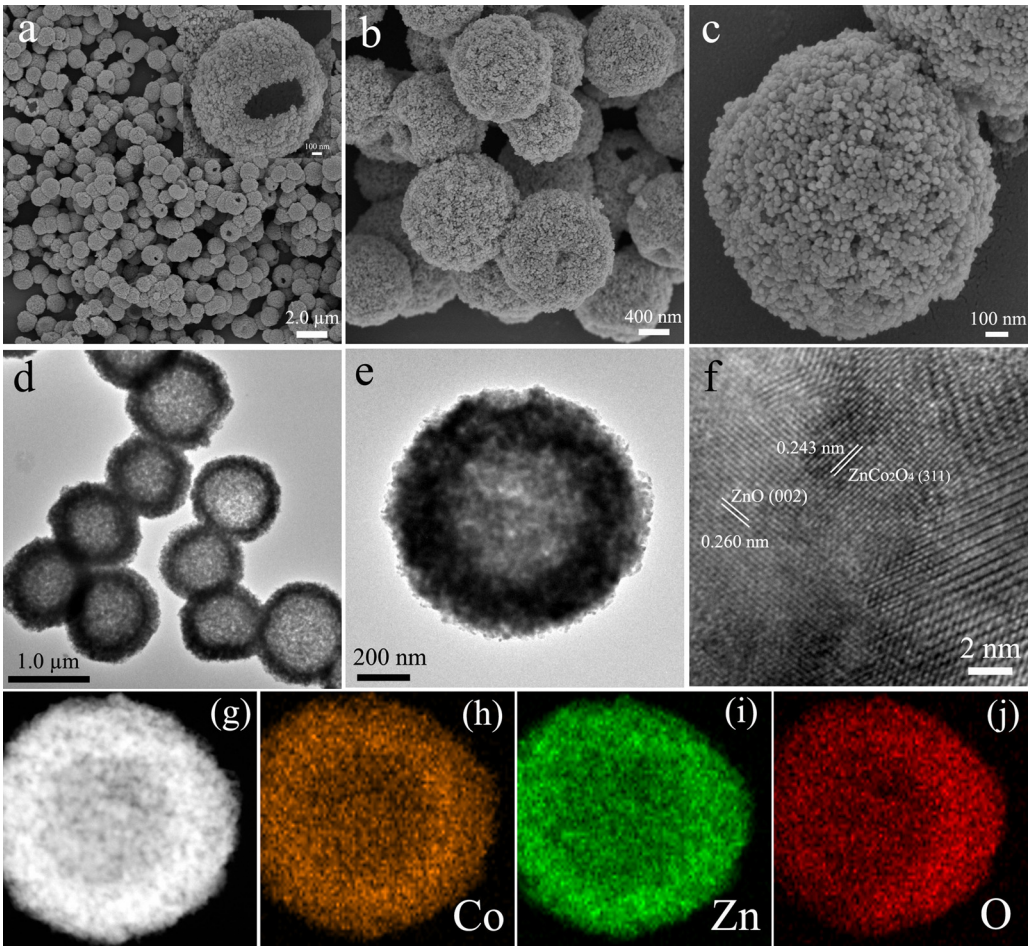

Fig. 3. The SEM (a-c), TEM (d-e) and HRTEM (f) images of ZnO–$ZnCo_2O_4$ hybrid hollow microspheres. The inset in (a) is a broken microsphere. STEM image (g) and the corresponding element mappings of Co (h), Zn (i) and O (j).

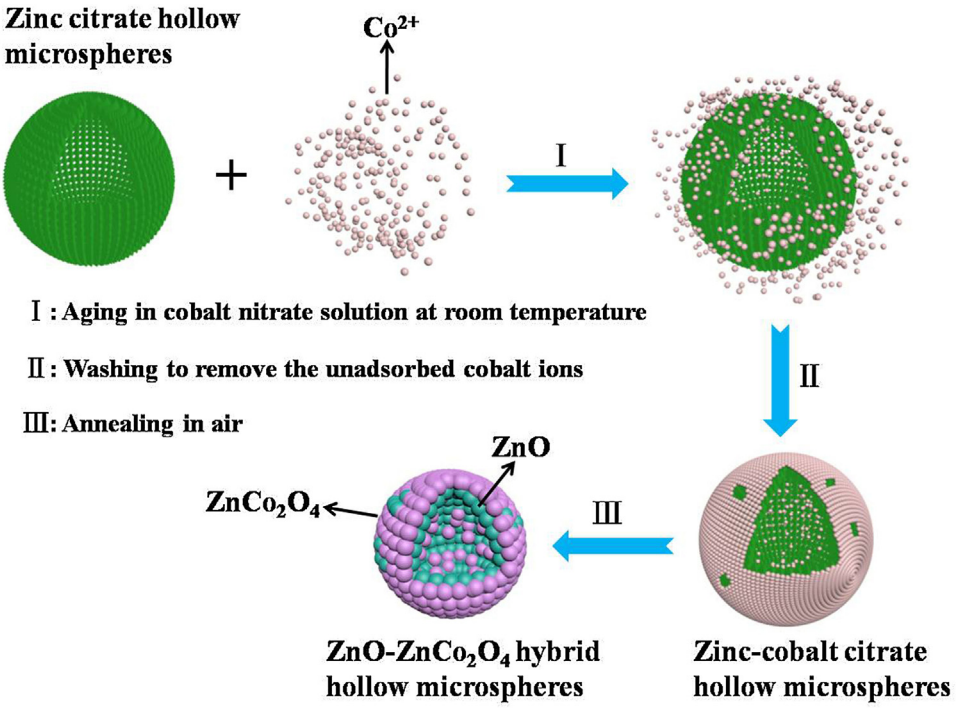

Fig. 4. Schematic diagram of the successful fabrication of well-dispersed ZnO–$ZnCo_2O_4$ hybrid hollow microspheres.

the formation of zinc–cobalt citrate hollow microspheres. By centrifugation and rinsing to remove the excess unadsorbed cobalt ions, the harvested zinc–cobalt citrate hollow microspheres are dried and then calcined at 500 °C in air. The adsorbed cobalt ions functioned as the cobalt sources would react with zinc citrate and oxygen to produce $ZnCo_2O_4$ during heating process. And the remanent zinc citrate would simultaneously convert to ZnO. Consequently, well-dispersed ZnO–$ZnCo_2O_4$ hybrid hollow microspheres can be synthesized. The intimate contact between ZnO and $ZnCo_2O_4$ nanoparticles is favorable to strengthen the electrochemical properties of hybrid hollow microspheres.

3.2. Electrochemical characterizations

Exhibited in Fig. 5a is the first three cyclic voltammogram (CV) curves of the ZnO–$ZnCo_2O_4$ hybrid hollow microspheres tested at 0.1 mV s^{-1} in 0.01–3 V, wherein two broad and strong cathodic peaks located at 0.83 and 0.40 V can be seen clearly in the first lithium intercalation process. The peak at 0.83 V derives from the decomposition of $ZnCo_2O_4$ to metallic Zn and Co, while the peak at 0.40 V is caused by the reduction of ZnO to metallic Zn, the formation of Zn–Li alloys together with the generation of solid electrolyte interphase (SEI) layers, which are in accordance with

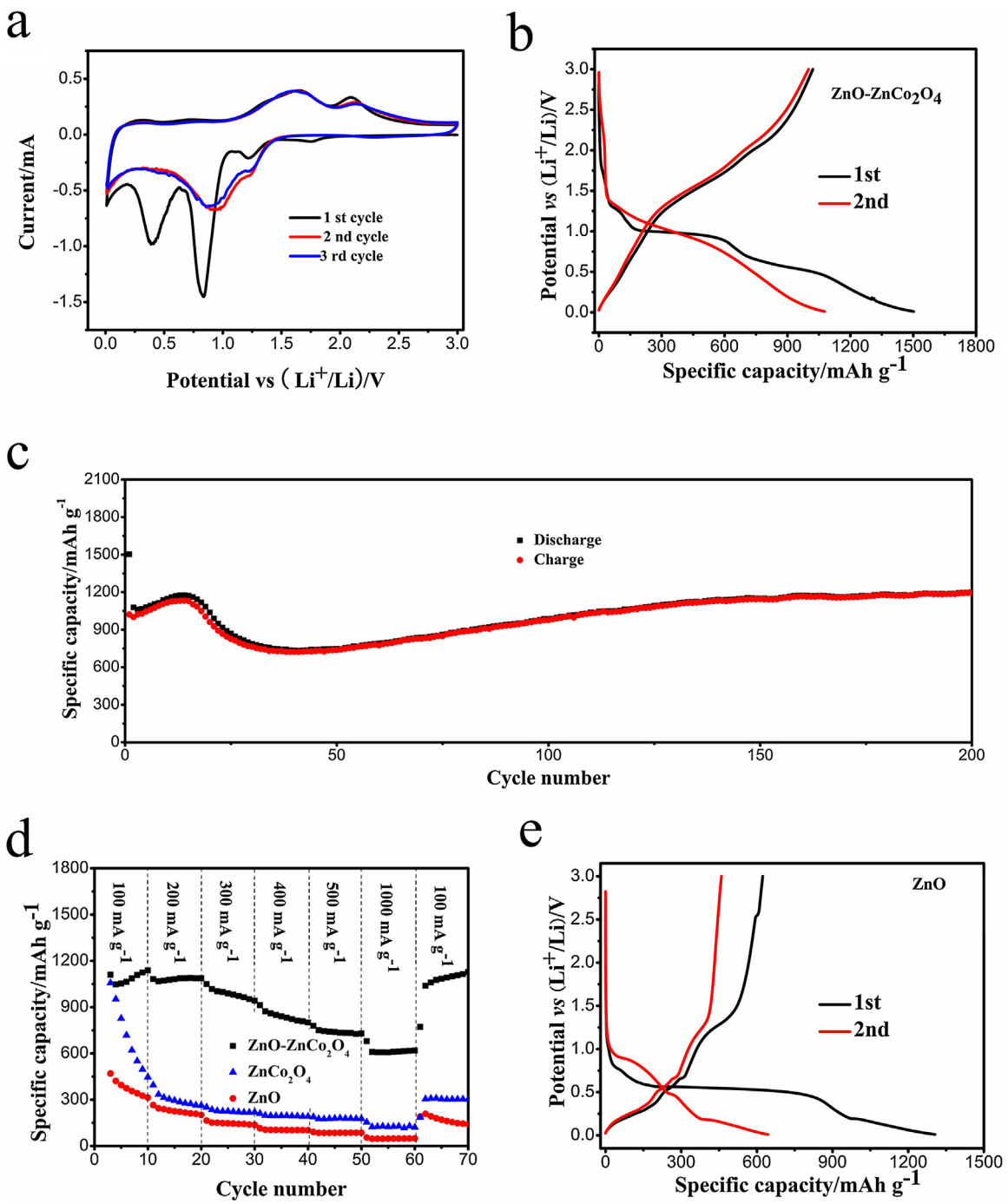

Fig. 5. The CV curves (a), galvanostatic discharge–charge profiles (b) and cycling performance (c) of ZnO–$ZnCo_2O_4$ hybrid hollow microspheres. (d) The rate capabilities of ZnO–$ZnCo_2O_4$, ZnO hollow microspheres and $ZnCo_2O_4$ nanoparticles. (e) The galvanostatic discharge-charge profiles of single ZnO hollow microspheres.

the previous reports [27,36]. In the first anodic scan, two weak peaks nearby 0.32 and 0.73 V relate to the multistep dealloying reactions of Zn–Li alloys. And the large peaks centered at 1.7 and 2.1 V are ascribed to formation of ZnO and Co_3O_4, respectively [27,37]. In the subsequent cathodic sweeps, the main reduction peak potential moves to larger value (0.95 V), which is caused by the changes in phase, crystallinity and structure of electrode materials during cycling [38]. From the second cycle onwards, apart from the slight differences in peak position, ZnO–$ZnCo_2O_4$ hybrids have similar CV curves in shape with other $ZnCo_2O_4$ electrode materials reported previously [22,37]. Chowdari's group fabricated four different $ZnCo_2O_4$ spherical particles by molten salt method and suggested that the slight differences in peak position in the CV curves of four $ZnCo_2O_4$ powders relate to their morphology and structures [22]. Additionally, in the second CV scan, the voltage hysteresis of ZnO and Co_3O_4 are about 0.7 and 1.2 V, respectively. The large voltage hysteresis of metal oxide electrodes on the basis of conversion reactions would greatly hinder their potential applications. Therefore, reducing the voltage hysteresis of the as-produced hybrid hollow microspheres is highly desirable. Previous reports have revealed that iron oxides electrodes possess slightly lower voltage hysteresis, thus fabricating ZnO–$ZnFe_2O_4$ hybrid hollow microspheres through the same method in our further work may be a good try to reduce the large voltage hysteresis [39–41]. In the subsequent cycles, the CV curves well superpose, indicative of the good reversibility of lithium storage. The electrochemical reactions of the hybrid hollow microspheres occurred during discharge/charge process are summarized as follows [22,36,39]:

$$ZnCo_2O_4 + 8\ Li^+ + 8\ e^- \rightarrow Zn + 2Co + 4\ Li_2O \quad (1)$$

$$ZnO + 2\ Li^+ + 2\ e^- \leftrightarrow Zn + Li_2O \quad (2)$$

$$Zn + x\ Li^+ + x\ e^- \leftrightarrow Li_xZn\ (x \leq 1) \quad (3)$$

$$Co + Li_2O \leftrightarrow CoO + 2\ Li^+ + 2\ e^- \quad (4)$$

$$CoO + 1/3\ Li_2O \leftrightarrow 1/3\ Co_3O_4 + 2/3\ Li^+ + 2/3\ e^- \quad (5)$$

The galvanostatic discharge–charge characterizations of ZnO–$ZnCo_2O_4$ hybrid hollow microspheres are implemented at 200 mA g^{-1} between 0.01–3.0 V and the corresponding results are depicted in Fig. 5b. The first discharge curve contains three obvious plateaus located at 1.30, 0.98 and 0.58 V, which are ascribed to the possible formation of SEI film, the decomposition of $ZnCo_2O_4$ to metallic Zn and Co, and the reduction of ZnO to Zn, respectively, being agreement with the above CV results. The hybrid hollow microspheres deliver the original discharge/charge capacities of 1503/1021 mA h g^{-1}, leading to a Coulombic efficiency of 64.8% which is higher than that (47.7%) of single ZnO hollow microspheres synthesized by directly annealing zinc citrate hollow microspheres in air (Fig. 5e). The irreversible capacity loss at the first cycle is possibly caused by the formation of SEI film [33]. Hong's group synthesized ZnO/$ZnCo_2O_4$ submicron rod arrays through an ammonia-evaporation-induced method, which delivered the first discharge/charge capacities of 1317/811 mA h g^{-1} [33]. ZnO–$ZnCo_2O_4$ hybrid hollow microspheres show extra-capacity of 180–350 mA h g^{-1} during the first cycle in comparison with ZnO/$ZnCo_2O_4$ submicron rod arrays. This phenomenon is common in other binary or ternary metal oxides electrodes and may be caused by the different preparation method of electrode materials [42,43]. The enhanced Coulombic efficiency of 93.1% in the second cycle indicates the increased reversibility of electrochemical reactions.

Fig. 5c demonstrates the cycling properties of ZnO–$ZnCo_2O_4$ hybrid hollow microspheres at 200 mA g^{-1} within 0.01–3.0 V. For comparison, the lithium storage properties of single ZnO hollow microspheres and $ZnCo_2O_4$ nanoparticles are also tested. Obviously, both ZnO hollow microspheres and $ZnCo_2O_4$ nanoparticles demonstrate the severe capacity degradation, indicating the poor cyclabilities (Fig. S6 and Fig. S7). After 60th cycles, the specific capacities of ZnO hollow microspheres and $ZnCo_2O_4$ nanoparticles are 149 and 448 mA h g^{-1}, respectively. Differently, the reversible capacity of ZnO–$ZnCo_2O_4$ hybrid hollow microspheres gradually increases in the first 15th cycles and then decreases with cycle number. From 40th cycle onwards, the reversible capacity increases again. After 200 cycles, ZnO–$ZnCo_2O_4$ hybrid hollow microspheres deliver a high specific capacity of about 1199 mA h g^{-1}, which is higher than the theoretical capacities of ZnO (978 mA h g^{-1}) and $ZnCo_2O_4$ (900 mA h g^{-1}). This phenomenon is associated with the reversible growth and dissolution of a polymeric gel-like film on the surface of the active materials during cycling, which would deliver extra specific capacity [44,45]. Undoubtedly, ZnO–$ZnCo_2O_4$ hybrid hollow microspheres show the greatly enhanced lithium storage properties compared to single ZnO hollow microspheres and $ZnCo_2O_4$ nanoparticles. To our knowledge, this is one of the best reversible capacities among various ZnO-based or $ZnCo_2O_4$-based electrode materials reported previously (Table 1). The rate capabilities of ZnO–$ZnCo_2O_4$ hybrid hollow microspheres, ZnO hollow microspheres and $ZnCo_2O_4$ nanoparticles are manifested in Fig. 5d. Apparently, ZnO–$ZnCo_2O_4$ hybrid hollow microspheres show the best rate capability than single ZnO hollow microspheres and $ZnCo_2O_4$ nanoparticles. The specific capacity of ZnO–$ZnCo_2O_4$ hybrid hollow microspheres gradually decreases with increasing the current density. A relatively high reversible capacity of about 618 mA h g^{-1} can be acquired even at a high current density of 1000 mA g^{-1}, which is still superior to traditional carbonaceous anode (372 mA h g^{-1}). Strikingly, the specific capacity gradually increases with cycle number when the current density returns to 100 mA g^{-1} and a high reversible capacity of 1128 mA h g^{-1} can be obtained after 70 cycles at this condition.

Table 1
The electrochemical properties of various ZnO- or $ZnCo_2O_4$-based electrode materials in lithium ion batteries.

Materials	Morphology	Reversible capacity /mAh g^1	Cycles	Ref.
ZnO–graphene	Nanocomposites	487	100	[46]
ZnO–C	Quantum Dots	1200	50	[47]
ZnO–C	Nanoparticles	654	100	[48]
ZnO–C	Yolk–shell/hollow/solid microspheres	520/427/341	150	[36]
ZnO–$ZnFe_2O_4$–C	Hollow octahedra	1390	100	[49]
$ZnCo_2O_4$	Core–shell/hollow/solid microspheres	985/831/345	50	[27]
$ZnCo_2O_4$	Mesoporous microspheres	721	80	[50]
$ZnCo_2O_4$–NiO	Nanowire arrays	357	50	[31]
$ZnCo_2O_4$–ZnO	Heterostructure rod arrays	900	30	[33]
ZnO–$ZnCo_2O_4$	Hybrid hollow microspheres	1199	200	Our work

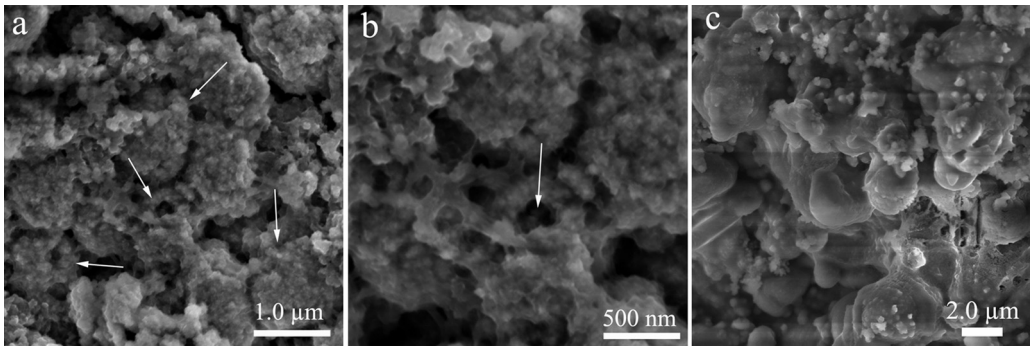

Fig. 6. The SEM images of ZnO–$ZnCo_2O_4$ hybrid hollow microspheres (a-b) and ZnO hollow microspheres (c) after 50th cycles. The arrows show the intact hybrid hollow microspheres.

The unique structural characteristics exert significant effect on the excellent lithium storage properties of the obtained ZnO–$ZnCo_2O_4$ hybrid hollow microspheres. First, the hollow structures of hybrid microspheres can offer extra space to mitigate the huge volume variation during the repetitive lithiation/delithiation process, which is capable of preventing the pulverizations of electrodes to some extent [9]. Second, the large surface area and the presence of mesopores in hybrid hollow microspheres would respectively offer more electrochemical active sites and favor the diffusion of electrolyte, consequently benefitting to increase the reversible capacity. Third, the shortened diffusion distance of lithium ions caused by the nanometer-sized building blocks of hybrid microspheres can strengthen the electrochemical reaction kinetics, which is beneficial to rate capability. Additionally, a polymeric gel-like layer would reversibly generate and dissolve at the surface of electrode materials owing to the nanometer-sized subunits features of hybrid microspheres, which can reinforce the reversible capacity of active materials [19,51]. Fourth, the synergetic effect between ZnO and $ZnCo_2O_4$ plays an important role in the good lithium storage properties of hybrid microspheres. ZnO and $ZnCo_2O_4$ nanoparticles well disperse within the whole hollow microspheres and contact with each other tightly. Both Zn and Co formed during discharge process would function as mutual beneficial matrices to effectively accommodate the severe volume change during lithium uptake/removal process, benefitting to the cyclability [25]. After 50 cycles, the microspherical structures of ZnO–$ZnCo_2O_4$ hybrids are kept well to a large extent, however, the single ZnO hollow microspheres have cracked to nanoparticles and then form the large aggregations (Fig. 6). The SEM observations well evidence the good structural tolerance of hybrid hollow microspheres. Fifth, it is well-established that Co nanocrystals formed during lithiation process show the catalytic effect to decompose Li_2O, which can contribute to extra specific capacity [52,53]. With all the merits mentioned above in mind, it is rational that the as-synthesized ZnO–$ZnCo_2O_4$ hybrid hollow microspheres demonstrate the high specific capacity, good cycling stability and superior rate capability.

4. Conclusions

In summary, zinc–cobalt citrate hollow microspheres are synthesized through a simple aging treatment and then calcined in air to successfully fabricate ZnO–$ZnCo_2O_4$ hybrid hollow microspheres. ZnO and $ZnCo_2O_4$ nanoparticles distribute homogeneously within the whole hollow microspheres and contact with each other closely. A high specific capacity, good cycling stability and superior rate performance are realized for the obtained hybrid hollow microspheres when applied as the anode materials for lithium ion batteries, which originate from the unique hollow configuration of hybrid microspheres, the nanometer-sized building blocks, the synergetic effect between ZnO and $ZnCo_2O_4$ as well as the catalytic effect of Co nanocrystals. Thus, the harvested ZnO–$ZnCo_2O_4$ hybrid hollow microspheres may be a good anode candidate for lithium ion batteries.

Acknowledgements

The authors gratefully acknowledge financial support from the National Basic Research Program of China (No. 2012CB933103), the National Natural Science Foundation of China (Grant Nos. 51171158 and 51371154) and the Fundamental Research Funds for the Central Universities of China (Grant no. 201312G003).

Appendix A. Supplementary data

Supplementary data associated with this article can be found, in the online version, at http://dx.doi.org/10.1016/j.electacta.2015.04.041.

References

[1] M. Armand, J.M. Tarascon, Building better batteries, Nature 451 (2008) 652–657.
[2] P. Meduri, E. Clark, E. Dayalan, G.U. Sumanasekera, M.K. Sunkara, Kinetically limited de-lithiation behavior of nanoscale tin-covered tin oxide nanowires, Energy Environ. Sci. 4 (2011) 1695–1699.
[3] Y. Lu, J.P. Tu, Q.Q. Xiong, J.Y. Xiang, Y.J. Mai, J. Zhang, Y.Q. Qiao, X.L. Wang, C.D. Gu, S.X. Mao, Controllable Synthesis of a Monophase Nickel Phosphide/Carbon (Ni_5P_4/C) Composite Electrode via Wet-Chemistry and a Solid-State Reaction for the Anode in Lithium Secondary Batteries, Adv. Funct. Mater. 22 (2012) 3927–3935.
[4] J.M. Tarascon, M. Armand, Issues and challenges facing rechargeable lithium batteries, Nature 414 (2001) 359–367.
[5] A.S. Arico, P. Bruce, B. Scrosati, J.M. Tarascon, W. Van Schalkwijk, Nanostructured materials for advanced energy conversion and storage devices, Nat. Mater. 4 (2005) 366–377.
[6] Y.J. Mai, S.J. Shi, D. Zhang, Y. Lu, C.D. Gu, J.P. Tu, NiO–graphene hybrid as an anode material for lithium ion batteries, J. Power Sources 204 (2012) 155–161.
[7] M.V. Reddy, G.V.S. Rao, B.V. Chowdari, Metal Oxides and Oxysalts as Anode Materials for Li Ion Batteries, Chem. Rev. 113 (2013) 5364–5457.
[8] J. Jiang, Y. Li, J. Liu, X. Huang, C. Yuan, X.W. Lou, Recent Advances in Metal Oxide-based Electrode Architecture Design for Electrochemical Energy Storage, Adv. Mater. 24 (2012) 5166–5180.
[9] Z. Wang, L. Zhou, X.W. Lou, Metal Oxide Hollow Nanostructures for Lithium-ion Batteries, Adv. Mater. 24 (2012) 1903–1911.
[10] C. Yuan, H.B. Wu, Y. Xie, X.W. Lou, Mixed Transition-Metal Oxides: Design, Synthesis, and Energy-Related Applications, Angew. Chem. Int. Ed. 53 (2014) 1488–1504.
[11] Q. Xie, Y. Ma, X. Zhang, H. Guo, A. Lu, L. Wang, G. Yue, D.L. Peng, Synthesis of amorphous $ZnSnO_3$-C hollow microcubes as advanced anode materials for lithium ion batteries, Electrochim. Acta 141 (2014) 374–383.
[12] X. Sun, C. Yan, Y. Chen, W. Si, J. Deng, S. Oswald, L. Liu, O.G. Schmidt, Three-Dimensionally Curved NiO Nanomembranes as Ultrahigh Rate Capability Anodes for Li-Ion Batteries with Long Cycle Life times, Adv. Energy Mater. 4 (2014) 1300912.

[13] Q. An, F. Lv, Q. Liu, C. Han, K. Zhao, J. Sheng, Q. Wei, M. Yan, L. Mai, Amorphous Vanadium Oxide Matrixes Supporting Hierarchical Porous Fe_3O_4/Graphene Nanowires as a High-Rate Lithium Storage Anode, Nano Lett. 14 (2014) 6250–6256.
[14] X. Sun, X. Wang, L. Qiao, D. Hu, N. Feng, X. Li, Y. Liu, D. He, Electrochemical behaviors of porous SnO_2–Sn/C composites derived from pyrolysis of SnO_2/poly(vinylidene fluoride), Electrochim. Acta 66 (2012) 204–209.
[15] M.V. Reddy, B. Zhang, J. Li, K. Zhang, B.V.R. Chowdari, Molten Salt Synthesis and Its Electrochemical Characterization of Co_3O_4 for Lithium Batteries, Electrochem. Solid-State Lett. 14 (2011) A79–A82.
[16] M.V. Reddy, G. Prithvi, K.P. Loh, B.V.R. Chowdari, Li Storage and Impedance Spectroscopy Studies on Co_3O_4 CoO, and CoN for Li-Ion Batteries, ACS Appl. Mater. Interfaces 6 (2014) 680–690.
[17] M.V. Reddy, C.T. Cherian, K. Ramanathan, K.C.W. Jie, T.Y.W. Daryl, T.Y. Hao, S. Adams, K.P. Loh, B.V.R. Chowdari, Molten synthesis of ZnO. Fe_3O_4 and Fe_2O_3 and its electrochemical performance, Electrochim. Acta 118 (2014) 75–80.
[18] X. Sun, W. Si, X. Liu, J. Deng, L. Xi, L. Liu, C. Yan, O.G. Schmidt, Multifunctional Ni/NiO hybrid nanomembranes as anode materials for high-rate Li-ion batteries, Nano Energy 9 (2014) 168–175.
[19] L. Zhou, D. Zhao, X.W. Lou, Double-Shelled $CoMn_2O_4$ Hollow Microcubes as High-Capacity Anodes for Lithium-Ion Batteries, Adv. Mater. 24 (2012) 745–748.
[20] C.T. Cherian, J. Sundaramurthy, M.V. Reddy, P.S. Kumar, K. Mani, D. Pliszka, C.H. Sow, S. Ramakrishna, B.V.R. Chowdari, Morphologically Robust $NiFe_2O_4$ Nanofibers as High Capacity Li-Ion Battery Anode Material, ACS Appl. Mater. Interfaces 5 (2013) 9957–9963.
[21] M.V. Reddy, C. Yu, F. Jiahuan, K.P. Loh, B.V.R. Chowdari, Molten salt synthesis and energy storage studies on $CuCo_2O_4$ and $CuO{\cdot}Co_3O_4$, RSC Adv. 2 (2012) 9619–9625.
[22] M.V. Reddy, K.Y.H. Kenrick, T.Y. Wei, G.Y. Chong, G.H. Leong, B.V.R. Chowdari, Nano-$ZnCo_2O_4$ Material Preparation by Molten Salt Method and Its Electrochemical Properties for Lithium Batteries, J. Electrochem. Soc. 158 (2011) A1423–A1430.
[23] M.V. Reddy, C.Y. Quan, K.W. Teo, L.J. Ho, B.V.R. Chowdari, Mixed Oxides, $(Ni_{1-x}Zn_x)Fe_2O_4$ (x = 0, 0. 25, 0. 5, 0. 75, 1): Molten Salt Synthesis, Characterization and Its Lithium-Storage Performance for Lithium Ion Batteries, J. Phys. Chem. C (2015) , doi:http://dx.doi.org/10.1021/jp5121178.
[24] A.S. Hameed, H. Bahiraei, M.V. Reddy, M.Z. Shoushtari, J.J. Vittal, C.K. Ong, B.V.R. Chowdari, Lithium Storage Properties of Pristine and (Mg, Cu) Codoped $ZnFe_2O_4$ Nanoparticles, ACS Appl. Mater. Interfaces 6 (2014) 10744–10753.
[25] Y. Sharma, N. Sharma, G.V.S. Rao, B.V.R. Chowdari, Nanophase $ZnCo_2O_4$ as a High Performance Anode Material for Li-Ion Batteries, Adv. Funct. Mater. 17 (2007) 2855–2861.
[26] W. Luo, X. Hu, Y. Sun, Y. Huang, Electrospun porous $ZnCo_2O_4$ nanotubes as a high-performance anode material for lithium-ion batteries, J. Mater. Chem. 22 (2012) 8916–8921.
[27] L. Huang, G.H. Waller, Y. Ding, D. Chen, D. Ding, P. Xi, Z.L. Wang, M. Liu, Controllable interior structure of $ZnCo_2O_4$ microspheres for high-performance lithium-ion batteries, Nano Energy 11 (2015) 64–70.
[28] B. Qu, L. Hu, Q. Li, Y. Wang, L. Chen, T. Wang, High-Performance Lithium-Ion Battery Anode by Direct Growth of Hierarchical $ZnCo_2O_4$ Nanostructures on Current Collectors, ACS Appl. Mater. Interfaces 6 (2014) 731–736.
[29] Q.Q. Xiong, J.P. Tu, X.H. Xia, X.Y. Zhao, C.D. Gu, X.L. Wang, A three-dimensional hierarchical Fe_2O_3@NiO core/shell nanorod array on carbon cloth: a new class of anode for high-performance lithium-ion batteries, Nanoscale 5 (2013) 7906–7912.
[30] S. Saadat, J. Zhu, D.H. Sim, H.H. Hng, R. Yazami, Q. Yan, Coaxial Fe_3O_4/CuO hybrid nanowires as ultra fast charge/discharge lithium-ion battery anodes, J. Mater. Chem. A 1 (2013) 8672–8678.
[31] Z. Sun, W. Ai, J. Liu, X. Qi, Y. Wang, J. Zhu, H. Zhang, T. Yu, Facile fabrication of hierarchical $ZnCo_2O_4$/NiO core/shell nanowire arrays with improved lithium-ion battery performance, Nanoscale 6 (2014) 6563–6568.
[32] J. Wang, Q. Zhang, X. Li, D. Xu, Z. Wang, H. Guo, K. Zhang, Three-dimensional hierarchical Co_3O_4/CuO nanowire heterostructure arrays on nickel foam for high-performance lithium ion batteries, Nano Energy 6 (2014) 19–26.
[33] C.W. Lee, S.D. Seo, D.W. Kim, S. Park, K. Jin, D.W. Kim, K.S. Hong, Heteroepitaxial growth of ZnO nanosheet bands on $ZnCo_2O_4$ submicron rods toward high-performance Li ion battery electrodes, Nano Research 6 (2013) 348–355.
[34] S.H. Choi, Y.C. Kang, Using Simple Spray Pyrolysis to Prepare Yolk-Shell-Structured ZnO-Mn_3O_4 Systems with the Optimum Composition for Superior Electrochemical Properties, Chem. Eur. J. 20 (2014) 1–6.
[35] Q. Xie, J. Li, Q. Tian, R. Shi, Template-free synthesis of zinc citrate yolk–shell microspheres and their transformation to ZnO yolk–shell nanospheres, J. Mater. Chem. 22 (2012) 13541–13547.
[36] Q. Xie, X. Zhang, X. Wu, H. Wu, X. Liu, G. Yue, Y. Yang, D.L. Peng, Yolk-shell ZnO-C microspheres with enhanced electrochemical performance as anode material for lithium ion batteries, Electrochim. Acta 125 (2014) 659–665.
[37] J. Li, J. Wang, D. Wexler, D. Shi, J. Liang, H. Liu, S. Xiong, Y. Qian, Simple synthesis of yolk-shelled $ZnCo_2O_4$ microspheres towards enhancing the electrochemical performance of lithium-ion batteries in conjunction with a sodium carboxymethyl cellulose binder, J. Mater. Chem. A 1 (2013) 15292–15299.
[38] M.V. Reddy, B. Zhang, K.P. Loh, B.V.R. Chowdari, Facile synthesis of Co_3O_4 by molten salt method and its Li-storage performance, CrystEngComm 15 (2013) 3568–3574.
[39] M.V. Reddy, G.V.S. Rao, B.V.R. Chowdari, Metal Oxides and Oxysalts as Anode Materials for Li Ion Batteries, Chem. Rev. 113 (2013) 5364–5457.
[40] B. Das, M.V. Reddy, B.V.R. Chowdari, Li-storage of Fe_3O_4/C composite prepared by one-step carbothermal reduction method, J.Alloys Compd. 565 (2013) 90–96.
[41] Y. Wu, P. Zhu, M.V. Reddy, B.V.R. Chowdari, S. Ramakrishna, Maghemite Nanoparticles on Electrospun CNFs Template as Prospective Lithium-Ion Battery Anode, ACS Appl. Mater. Interfaces 6 (2014) 1951–1958.
[42] M.V. Reddy, C. Yu, J. Fan, K.P. Loh, B.V.R. Chowdari, Li-Cycling Properties of Molten Salt Method Prepared Nano/Submicrometer and Micrometer-Sized CuO for Lithium Batteries, ACS Appl. Mater. Interfaces 5 (2013) 4361–4366.
[43] C.T. Cherian, M.V. Reddy, G.V.S. Rao, C.H. Sow, B.V.R. Chowdari, Li-cycling properties of nano-crystalline $(Ni_{1-x}Zn_x)Fe_2O_4$ $(0 \leq x \leq 1)$, J.Solid State Electrochem. 16 (2012) 1823–1832.
[44] S. Xu, C.M. Hessel, H. Ren, R. Yu, Q. Jin, M. Yang, H. Zhao, D. Wang, α-Fe_2O_3 multi-shelled hollow microspheres for lithium ion battery anodes with superior capacity and charge retention, Energy Environ. Sci. 7 (2014) 632–637.
[45] S.H. Choi, Y.C. Kang, Yolk-Shell, Hollow, and Single-Crystalline $ZnCo_2O_4$ Powders: Preparation Using a Simple One-Pot Process and Application in Lithium-Ion Batteries, ChemSusChem 6 (2013) 2111–2116.
[46] M. Yu, A. Wang, Y. Wang, C. Li, G. Shi, An alumina stabilized ZnO-graphene anode for lithium ion batteries via atomic layer deposition, Nanoscale 6 (2014) 11419–11424.
[47] S.J. Yang, S. Nam, T. Kim, J.H. Im, H. Jung, J.H. Kang, S. Wi, B. Park, C.R. Park, Preparation and exceptional lithium anodic performance of porous carbon-coated ZnO quantum dots derived from a metal-organic framework, J. Am. Chem. Soc. 135 (2013) 7394–7397.
[48] X. Shen, D. Mu, S. Chen, B. Wu, F. Wu, Enhanced electrochemical performance of ZnO-loaded/porous carbon composite as anode materials for lithium ion batteries, ACS Appl. Mater. Interfaces 5 (2013) 3118–3125.
[49] F. Zou, X. Hu, Z. Li, L. Qie, C. Hu, R. Zeng, Y. Jiang, Y. Huang, MOF-Derived Porous ZnO/$ZnFe_2O_4$/C Octahedra with Hollow Interiors for High-Rate Lithium-Ion Batteries, Adv. Mater. 26 (2014) 6622–6628.
[50] L. Hu, B. Qu, C. Li, Y. Chen, L. Mei, D. Lei, L. Chen, Q. Li, T. Wang, Facile synthesis of uniform mesoporous $ZnCo_2O_4$ microspheres as a high-performance anode material for Li-ion batteries, J. Mater. Chem. A 1 (2013) 5596–5602.
[51] P.G. Bruce, B. Scrosati, J.M. Tarascon, Nanomaterials for rechargeable lithium batteries, Angew. Chem. Int. Ed. 47 (2008) 2930–2946.
[52] W.S. Kim, Y. Hwa, H.C. Kim, J.H. Choi, H.J. Sohn, S.H. Hong, SnO_2@Co_3O_4 hollow nano-spheres for a Li-ion battery anode with extraordinary performance, Nano Research 7 (2014) 1128–1136.
[53] Y.M. Kang, M.S. Song, J.H. Kim, H.S. Kim, M.S. Park, J.Y. Lee, H.K. Liu, S.X. Dou, A study on the charge–discharge mechanism of Co_3O_4 as an anode for the Li ion secondary battery, Electrochim. Acta 50 (2005) 3667–3673.